Recombining Your Way Out of Trouble: The Genetic Architecture of Hybrid Fitness under Environmental Stress

Zebin Zhang,[†,1] Devin P. Bendixsen ,[†,1] Thijs Janzen,[2,3] Arne W. Nolte,[2,3] Duncan Greig,[2,4] and Rike Stelkens [*,1,2]

[1]Division of Population Genetics, Department of Zoology, Stockholm University, Stockholm, Sweden

[2]Max Planck Institute for Evolutionary Biology, Plön, Germany

[3]Institute of Biology and Environmental Sciences, University of Oldenburg, Oldenburg, Germany

[4]Centre for Life's Origins and Evolution (CLOE), Department of Genetics, Evolution, and Environment, University College London, London, United Kingdom

[†]These authors contributed equally to this work.

***Corresponding author:** E-mail: rike.stelkens@zoologi.su.se.

Associate editor: Aya Takahashi

Abstract

Hybridization between species can either promote or impede adaptation. But we know very little about the genetic basis of hybrid fitness, especially in nondomesticated organisms, and when populations are facing environmental stress. We made genetically variable F2 hybrid populations from two divergent *Saccharomyces* yeast species. We exposed populations to ten toxins and sequenced the most resilient hybrids on low coverage using ddRADseq to investigate four aspects of their genomes: 1) hybridity, 2) interspecific heterozygosity, 3) epistasis (positive or negative associations between nonhomologous chromosomes), and 4) ploidy. We used linear mixed-effect models and simulations to measure to which extent hybrid genome composition was contingent on the environment. Genomes grown in different environments varied in every aspect of hybridness measured, revealing strong genotype–environment interactions. We also found selection against heterozygosity or directional selection for one of the parental alleles, with larger fitness of genomes carrying more homozygous allelic combinations in an otherwise hybrid genomic background. In addition, individual chromosomes and chromosomal interactions showed significant species biases and pervasive aneuploidies. Against our expectations, we observed multiple beneficial, opposite-species chromosome associations, confirmed by epistasis- and selection-free computer simulations, which is surprising given the large divergence of parental genomes (∼15%). Together, these results suggest that successful, stress-resilient hybrid genomes can be assembled from the best features of both parents without paying high costs of negative epistasis. This illustrates the importance of measuring genetic trait architecture in an environmental context when determining the evolutionary potential of genetically diverse hybrid populations.

***Key words:* *Saccharomyces*, hybridization, environmental stress, ddRADseq, heterozygosity, epistasis, genome evolution.**

Article

Introduction

Populations exposed to gene flow, introgression, or hybridization contain vast amounts of genetic variation, sometimes producing phenotypes with more extreme adaptations than found in the parent populations (Shahid et al. 2008; Stelkens and Seehausen 2009; Pritchard et al. 2013; Stelkens, Brockhurst, Hurst, Miller, et al. 2014; Holzman and Hulsey 2017). The average fitness of hybrid crosses is usually lower than that of nonhybrid crosses due to interspecific incompatibilities or other negative effects, for example, the break-up and loss of coadapted beneficial gene complexes for local adaptation (Coyne and Orr 2004). This applies especially to the hybrid offspring of genetically divergent lineages. However, some hybrids show high fitness (Rieseberg et al. 1999; Dittrich-Reed and Fitzpatrick 2013), which is often exploited in agricultural breeding to improve the yield, taste, or other desirable traits of cultivars (Marullo et al. 2006; Kuczyńska et al. 2007; Shivaprasad et al. 2012; Koide et al. 2019). But fit and fertile hybrids are also relevant for adaptive evolution and the generation of biodiversity, especially when ecologically divergent hybrid phenotypes become reproductively isolated from the parents. Ultimately this process can lead to hybrid speciation (Anderson and Stebbins 1954; Lewontin and Birch 1966; Rieseberg et al. 2003; Seehausen 2004; Arnold 2006; Mallet 2007; Nolte and Tautz 2010; Abbott et al. 2013; Schumer et al. 2014).

The genetic mechanisms allowing some hybrid genomes to express high-fitness phenotypes, despite negative epistatic effects compromising their fitness, are poorly known, especially in nondomesticated organisms. We also know very little

about the impact of stressful and deteriorating environmental conditions on the evolutionary potential of hybrid populations, although this is becoming increasingly relevant in the face of global environmental change and invasive species management. So far, empirical studies putting hybrid fitness in an environmental context are rare and the results are mixed. Some found environmental stress to intensify the negative fitness effects of hybridization (Koevoets et al. 2012; Barreto and Burton 2013), others found hybrid fitness to increase with stress (Edmands and Deimler 2004; Willett 2012; Hwang et al. 2016). Again, others detected no effects of stress on hybrid fitness (Armbruster et al. 1999). Studies in interspecific yeast crosses suggest that F2 hybrids can outcompete their parent species in various stressful environments (Greig et al. 2002; Stelkens, Brockhurst, Hurst, and Greig 2014) and that hybridization can increase resistance against a range of toxins (Stelkens, Brockhurst, Hurst, Miller, et al. 2014).

We made genetically highly variable F2 hybrids by crossing two divergent species of *Saccharomyces* budding yeast (*S. cerevisiae* and *S. paradoxus*). These species have well-sequenced, well-assembled genomes that differ at ~15% of nucleotides genome-wide (Liti et al. 2009). Due to their large divergence, these species produce only ~1% viable F2-hybrid offspring (Hunter et al. 1996; Boynton et al. 2018; Rogers et al. 2018). We exposed 240 populations of viable F2 hybrids to ten stressful environments containing high concentrations of different toxins (e.g., caffeine, ethanol, lithium acetate; supplementary table S1, Supplementary Material online). At the end of the growth period, we sequenced the genomes of 240 hybrid survivors at low coverage using double digest, restriction-site-associated DNA (ddRAD) markers and mapped hybrid genomes to both parental reference genomes to analyze their genome composition. To measure the impact of the genetic and environmental factors shaping the hybrid genomes, we measured four aspects of "hybridness"; 1) hybridity (proportion of hybrid genome mapping to one or other parent species), 2) interspecific heterozygosity (homologous chromosomes from opposite species), 3) epistasis (positive or negative associations between nonhomologous chromosomes from the same and opposite species), and aneuploidy (aberrant chromosome copy numbers compared with the euploid parents). By virtue of design, we were restricted to sampling only from the 1% viable subset of F2 hybrids here (i.e., we could only sequence survivors and not the inviable hybrids carrying lethal incompatibilities).

Hybridity is a continuous measure. It is the proportion of genomic material inherited from one over the other parental species (Gompert and Buerkle 2016), often referred to as hybrid index (Barton and Gale 1993; Buerkle 2005) or admixture proportion (Pritchard et al. 2000; Falush et al. 2003). Hybridity is useful for locating hybrid genomes on a single axis, ranging from zero to one with pure parental genomes at opposite ends. However, this simple measure can mask potentially important fitness effects of individual loci (or chromosomes) deviating from the average hybridity of the genome. For instance, dominance (the reciprocal masking of deleterious alleles at multiple loci; Bruce 1910) and overdominance (the intrinsic benefit of being heterozygous for at least one locus) can produce hybrids with high fitness. This is known as "interspecific heterozygosity" or "interpopulation ancestry" (Barton 2000; Fitzpatrick 2012; Lindtke et al. 2012; Gompert and Buerkle 2013). As an example, although every chromosome in a diploid F1 hybrid is heterozygous, maximizing within-locus hybridity, the genome still carries a full haploid set of both parental chromosomes. At the same time, a diploid F2 or higher generation hybrid can, theoretically, be composed of fully homozygous chromosomes (i.e., homologous chromosomes are from the same species), which minimizes within-locus hybridity. But this F2 hybrid may contain half the chromosomal set from either parent, maximizing between-locus hybridity. Because these types of hybrids would be indistinguishable with a single hybrid index (which would be 0.5 in both examples), we also measured interspecific heterozygosity, that is, chromosomes in the F2 hybrid genome carrying interspecific, homologous combinations.

Epistasis, caused by interactions between alleles from at least two different loci that increase or decrease fitness more than the sum of the individual contributions of these loci, is common in nature and has been shown to be susceptible to changes in the environment (Kvitek and Sherlock 2011; de Vos et al. 2013). Jaffe et al. (2019) showed that adding more environmental conditions tripled the number of genetic interactions detected in fitness assays between double mutants of yeast (Jaffe et al. 2019). Filteau et al. (2015) found that the course of compensatory evolution rescuing yeast populations from the negative fitness effects of deleterious mutations was strongly contingent on the environment (different carbon sources) (Filteau et al. 2015). Lee et al. (2019), dissecting the genetic basis of a yeast colony phenotype, recently found that environmental stress affected the impact of epistasis, additivity, and genotype–environment interactions.

Epistasis, especially negative epistasis, is predicted to play a large role in hybrid fitness (Cubillos et al. 2011; Shapira et al. 2014). Negative epistasis is the core element of the Dobzhansky–Muller model of genetic incompatibilities (DMIs), which is often recruited to explain the evolution of reproductive isolation and outbreeding depression between biological species, with increasing negative impact the more divergent the parental genomes are (Dobzhansky 1936; Müller 1942; Lynch 1991). Here, we measured epistasis by testing for significant associations (presence and absence) between nonhomologous chromosomes from different species in F2 hybrid yeast genomes. We compared our data with epistasis- and selection-free simulations, assuming free segregation of chromosomes in a theoretical F2 hybrid population. Given the large nucleotide divergence between the parental genomes used here (~15% genome-wide), negative epistasis is expected to be prominent, and we expected to find more same species associations than opposite species associations in F2 hybrids. However, it is important to keep in mind that we were restricted to sampling only from the viable subset of F2 hybrids here (because we cannot sequence dead hybrids). As a result, we cannot make inferences about the impact of DMIs on the average fitness of this hybrid cross, and our results remain inconclusive as to the relative importance of DMIs compared with other genetic mechanisms of hybrid

breakdown, such as underdominance, or directional selection for one of the parental alleles in hybrid genomes.

Results

We sequenced a total of 240 F2 hybrid strains, of which 184 were mostly diploid and 53 were mostly haploid (three genomes were discarded due to low read quality). Thus, the majority of spores germinated and mated in the 96-well plates, forming diploid F2 hybrids homozygous for both drug resistance markers *cyh2r* and *can1r*. The haploid genotypes detected by sequencing were unmated F2 (i.e., F1 spores), and hemizygous for *cyh2r* and *can1r*. Because we saw no significant differences between F2 samples isolated from high concentration of a toxin and low concentration in any of the tests, we proceeded by pooling all samples for analysis.

Interspecific Heterozygosity

To measure interspecific heterozygosity (i.e., genomes having homologous chromosomes from both species) in our diploid samples, we considered chromosomes heterozygous if marker proportions fell between 0.25 and 0.75. Chromosomes with smaller or larger species content were considered homozygous for the dominant species. Assuming no selection and free segregation of chromosomes in our simulated chromosomes, interspecific heterozygosity was lower than expected in the 187 diploid F2 genomes across all toxins (mean heterozygosity = 0.44, median = 0.36; fig. 1A). This low level of mean heterozygosity was found in <0.8% of simulations based on no interactions (supplementary fig. S1, Supplementary Material online). On average, only 7 of the 16 chromosomes per genome carried a heterospecific combination. In total, there were almost 1.3 times more homozygous chromosomes ($n = 1{,}450$; 57%) than heterozygous chromosomes ($n = 1{,}126$; 43%). Environments differed substantially in the proportions of homo- and heterozygous chromosomes (fig. 1B). Although in some environments, F2 hybrids were mainly homozygous (e.g., zinc sulfate: 0.73), other environments promoted the growth of mainly heterozygote genotypes (e.g., NaCl: 0.56). This was confirmed using simulations. Five stress environments (zinc sulfate: 0.28, citric acid: 0.29, ethanol: 0.32, salicylic acid: 0.35, and caffeine: 0.40) produced mean interspecific heterozygosities below the range (0.41–0.59) expected based on random segregation simulations (supplementary fig. S1, Supplementary Material online). Seven environments produced mean homozygosities above the expected range: Three environments (zinc sulfate: 0.35, citric acid: 0.35, and ethanol: 0.36) produced F2 genomes more homozygous than the simulated range (0.16–0.34) of expected homozygosity for *S. cerevisiae*. Four environments (caffeine: 0.33, citric acid: 0.36, salicylic acid: 0.37, and zinc sulfate: 0.37) produced F2 genomes with higher homozygosity than the simulated range (0.15–0.33) of expected homozygosity for *S. paradoxus*.

Testing for variation in zygosity between chromosomes, across all environments, we found three chromosomes with a significantly larger proportion of *S. cerevisiae* homozygotes (chromosomes 4: 0.57, 5: 0.31, 14: 0.78), and three chromosomes with a significantly larger proportion of *S. paradoxus* homozygotes (chromosomes 6: 0.45, 7: 1.0, 10: 0.36; fig. 1C). Note that chromosomes 5 and 7 carried resistance genes, which, as predicted, selected them to be homozygous for *S. cerevisiae* and *S. paradoxus*, respectively (chromosome 5 also carried some *S. paradoxus* content due to recombination at one end of the chromosome). Three chromosomes were more often heterozygous than expected by chance (chromosomes 2: 0.60, 3: 0.56, 12: 0.58).

Using a linear mixed-effect model to understand what causes variation in zygosity between environments, chromosomes, and genomes, we found that the interaction between *chromosome ID* and *environment* best predicted zygosity (supplementary table S2, Supplementary Material online). Thus, which chromosome was homozygous, and which chromosome was heterozygous, was largely determined by the stress environment from which it was sampled.

Chromosome Copy Number

To quantify the chromosome copy number within all F2 genomes and to detect potential aneuploidies, we considered a chromosome aneuploid if the mean copy number was >2.5 or <1.5 in diploids, and >1.5 in haploids. Using this cut-off, we found that 47 overall haploid genomes and 161 overall diploid genomes of the 237 F2 hybrids contained aneuploidy, affecting 15.3% of all chromosomes in haploids and 14.8% of chromosomes in diploids (i.e., on average 2.4 chromosomes per genome were aneuploid; supplementary fig. S2*A*, Supplementary Material online). Although no significant differences were detected between overall chromosome copy numbers of F2 hybrids and euploid F1 hybrids within environments (Wilcoxon test; supplementary fig. S2*B*, Supplementary Material online), using data from all environments, we found significant differences between chromosomes in average copy number, with nine chromosomes (1, 4, 5, 6, 7, 8, 12, 13, and 14) having significantly different ploidy from the chromosomes in euploid F1 genomes (supplementary fig. S2*C*, Supplementary Material online). For instance, chromosomes 2, 4, 13, and 14 showed high percentages of aneuploidy, whereas chromosomes 5 and 7 showed low percentages, probably due to the drug marker they contained (supplementary fig. S2*D*, Supplementary Material online). Supplementary figure S3, Supplementary Material online, provides an overview of the pervasive aneuploidy we found in the F2 hybrid genomes in ten stressful environments. Supplementary figure S4, Supplementary Material online, shows the chromosome copy number of one representative aneuploid F2 hybrid genome chosen from each environment for illustration.

Genome-Wide Hybridity

Average genome-wide hybridity (defined to be the percentage of markers inherited from *S. cerevisiae*) was 0.52 ± 0.05 ($\mu \pm$SD) across all chromosomes and all environments (supplementary fig. S5*A*, Supplementary Material online). This pattern was consistent with the analysis of published data (Kao et al. 2010) from an environment without added stress (supplementary fig. S6*A*, Supplementary Material online). Thus, genomic contributions were roughly balanced between

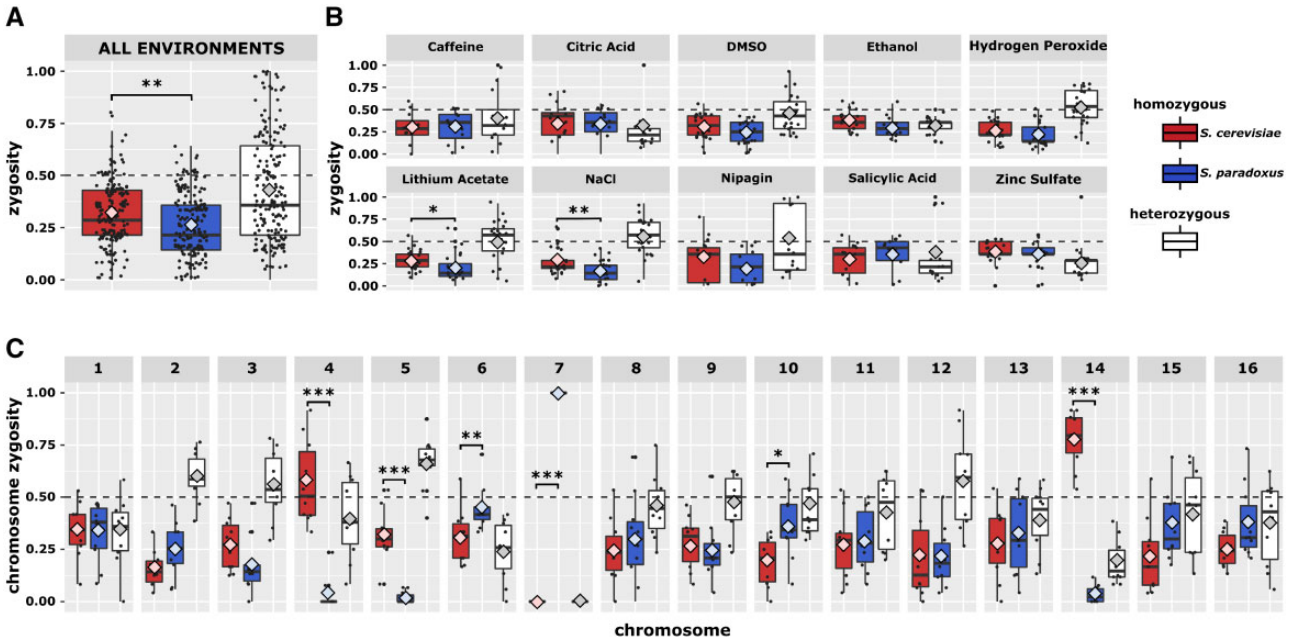

FIG. 1. Homo-/heterozygosity of diploid F2 hybrid genomes. (*A*) Mean zygosity of 187 diploid F2 hybrids across all chromosomes (except chromosomes 5 and 7) and across all environments. Dashed horizontal line (at 0.5) shows expected heterozygosity without selection and free segregation. Black lines in boxes are medians and large diamonds indicate means. Each black dot represents a genome. Boxes are interquartile ranges (IQR). Whiskers are 1.5 × IQR. (*B*) Mean F2 hybrid zygosity per environment. (*C*) Mean F2 hybrid zygosity per chromosome. Chromosomes 5 and 7 harbor drug markers selecting for *Saccharomyces cerevisiae* and *S. paradoxus* chromosomes, respectively. Each dot represents one of ten environments. Asterisks indicate significant differences in proportions of *S. cerevisiae* versus *S. paradoxus* homozygotes in Wilcoxon signed-rank tests (P = *0.05, **0.01, ***0.001).

the two parental species with a slight overrepresentation of *S. cerevisiae*. The most biased genome toward *S. cerevisiae* was 0.68 and the most biased toward *S. paradoxus* was 0.35. Average hybridity per toxin ranged from 0.49 ± 0.07 in salicylic acid (*paradoxus*-biased) to 0.55 ± 0.07 (*cerevisiae*-biased) in Nipagin, but no significant differences were found between toxins (supplementary fig. S5*B*, Supplementary Material online). The distributions and means of genome-wide hybridity observed in each environment were all within the range (0.44–0.56) expected from simulations based on random chromosome segregation (supplementary fig. S7, Supplementary Material online). Chromosomes 5 and 7 were excluded from these analyses because they carried antibiotic resistance markers selecting for *S. cerevisiae* and *S. paradoxus* hemi- or homozygosity, respectively.

Chromosome Hybridity

A closer examination of hybridity (defined to be % markers inherited from *S. cerevisiae*) at the chromosomal level revealed species biases in inheritance patterns (fig. 2*A*). For most chromosomes the average chromosome hybridity across all environments was ~0.5, suggesting equal inheritance from *S. cerevisiae* and *S. paradoxus*. As expected, chromosome 5 was inherited primarily from *S. cerevisiae* and chromosome 7 was inherited primarily from *S. paradoxus* because they carried species-specific drug markers. Interestingly, chromosomes 4 and 14 were also inherited predominantly from *S. cerevisiae* (0.77 and 0.88, respectively). Analysis of previously published data in an environment without stress (Kao et al. 2010) also found this bias in chromosome 4 (supplementary fig. S6*B*, Supplementary Material online). Nine of the 16 chromosomes exhibited varying levels of hybridity depending on environment (ANOVA, $P < 0.05$), with six showing significant variation (fig. 2*B*, $P < 0.001$). For some chromosomes, the hybridity variation resulting from environment did not change the species bias (chromosomes 7 and 14). However, some chromosomes shifted from unbiased (~0.5 hybridity) to biased for *S. paradoxus* in some environments (chromosomes 10 and 15). Two chromosomes exhibited opposite species biases depending on the environment (chromosomes 12 and 13). In some environments these chromosomes were biased toward *S. cerevisiae* (>0.65%), and in other environments they were biased toward *S. paradoxus* (<0.35%).

Using a linear mixed-effect model, we found that interactions between *aneuploidy* and *environment*, *chromosome ID* and *environment*, and *aneuploidy*, *chromosome ID* and *ploidy* (haploid or diploid) best predicted the hybridity of the chromosome (supplementary table S3, Supplementary Material online). The optimal model did not change if data from chromosomes 5 and 7 were excluded.

By combining our chromosome hybridity data with published "relative fitness" data for the parental strains in each environment (Bernardes et al. 2017), we found a possible link between species-biased chromosomal inheritance and parental fitness. We derived "parental phenotypic divergence" from Bernardes et al. (supplementary fig. S8*A*, Supplementary Material online), defined as the difference between the competitive growth of the two parents relative to their

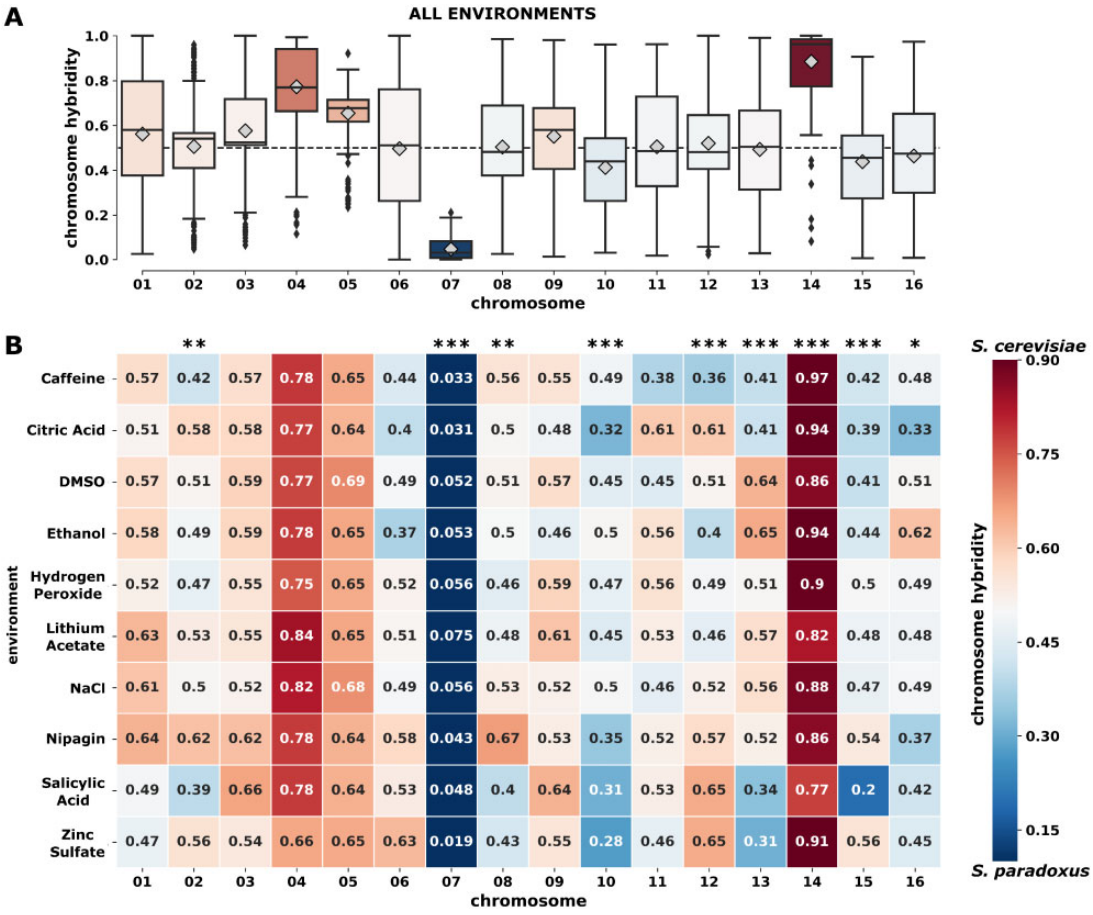

FIG. 2. Chromosome hybridity of 237 haploid and diploid F2 genomes. (*A*) Chromosome hybridity for each chromosome across all environments. Chromosome hybridity is measured as the percent chromosome mapping to *Saccharomyces cerevisiae*. Boxplots as in figure 1, but colored according to where the median falls. Dashed line (0.5) indicates equal amounts of the chromosome mapping to *S. cerevisiae*. Species biases on chromosomes 5 (~65% from *S. cerevisiae*) and 7 (~5% from *S. cerevisiae*) are by design and result from alternative recessive drug markers. (*B*) Chromosome hybridity for each chromosome within environments. Numbers in colored boxes indicate average chromosome hybridity across 24 F2 diploid genomes. Asterisks indicate significant differences in average chromosome hybridity across environments (P = *0.05, **0.01, ***0.001).

interspecific F1 hybrid (*S. cerevisiae*–*S. paradoxus*). Negative parental phenotypic divergence suggests that the *S. cerevisiae* parent performed better in competition with the hybrid. Positive parental phenotypic divergence suggests that the *S. paradoxus* parent performed better during competition with the hybrid. Note that parental phenotypic divergence is a relative measure here and assumes transitivity of relative fitness between each of the two parents and the F1 hybrid. This analysis revealed a significant correlation ($P < 0.05$) between parental phenotypic divergence and chromosome hybridity in chromosomes 1 and 13 (supplementary fig. S8*B*, Supplementary Material online). This relationship suggests that in environments with a higher relative fitness for the *S. cerevisiae* parent, chromosome hybridity was biased toward *S. cerevisiae*. Inversely, in environments with higher relative fitness for the *S. paradoxus* parent, chromosome hybridity was biased toward *S. paradoxus*.

Chromosome Hybridity Interactions

Testing for chromosomal hybridity interactions within a given F2 genome revealed strong environment-dependent effects. A large difference in chromosome hybridity for each chromosome combination, defined as delta chromosome hybridity (DCH), indicated that two chromosomes mapped primarily to opposing species within a given F2 genome. This could potentially result from negative epistatic interactions within species (i.e., chromosome incompatibility), from positive epistatic interactions between species or a combination of the two. Some chromosomes maintained high DCH suggesting that they were preferably from opposing species across all environments (fig. 3*A*, chr7 × chr4, chr7 × chr14, chr7 × chr5). Chromosome 7 and 5 were designed to come from opposing species and were therefore expected to have high DCH. However, the remaining high DCH interactions with chromosome 7 suggest potential chromosome incompatibilities or strong positive epistatic interactions between species. Chromosome 7 was designed to be inherited from *S. paradoxus* and potentially resulting from this, chromosome 4 and chromosome 14 were primarily inherited from *S. cerevisiae*. Analyzing the DCH in each stress environment independently showed that different environments exhibited varying levels and distributions of DCH (fig. 3*B*). Two environments (zinc sulfate: 0.37, salicylic acid: 0.39) exhibited higher mean DCH than the

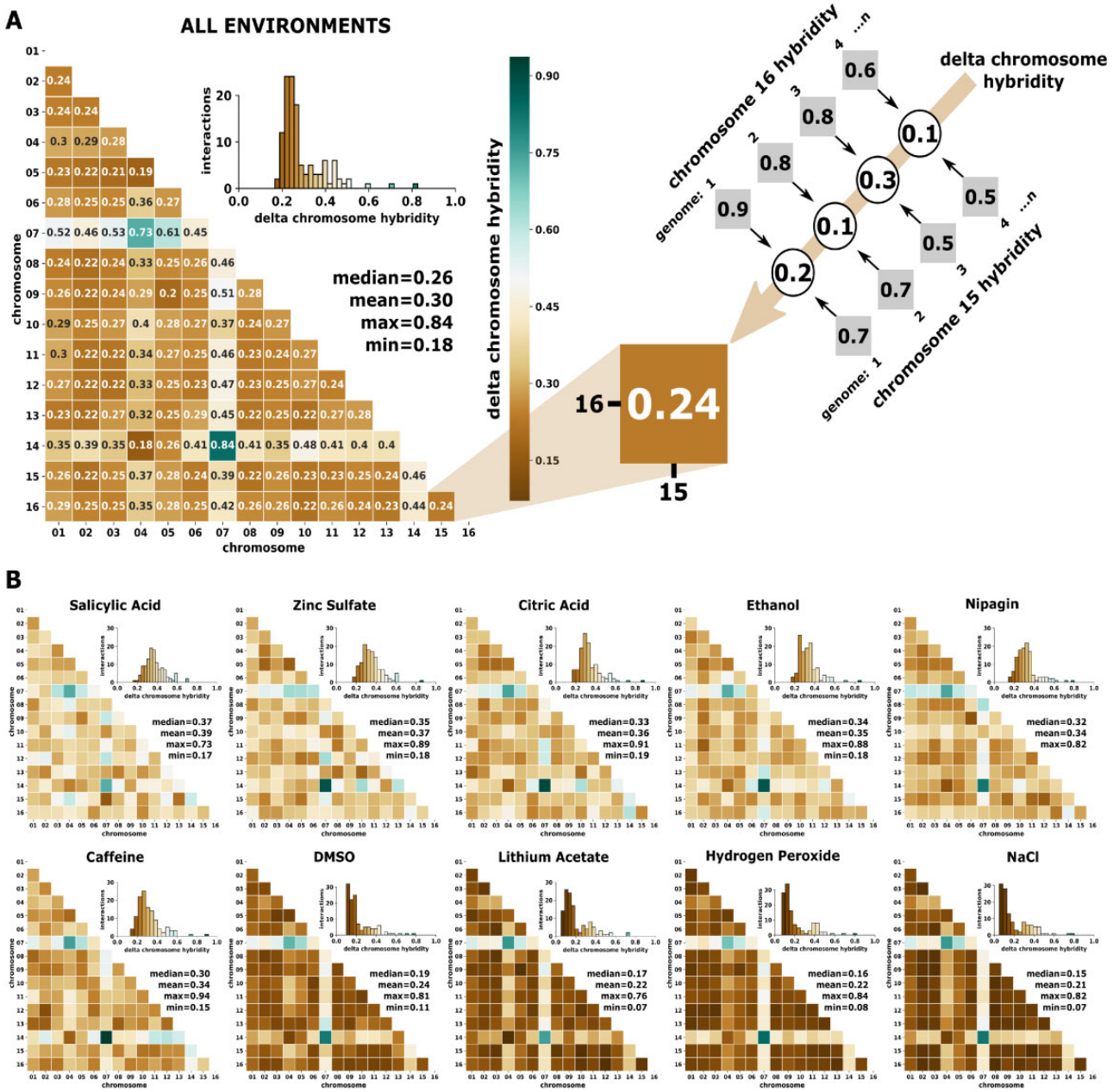

FIG. 3. Interactions of chromosome hybridities altered by environment. (*A*) Average change in chromosome hybridity (percent chromosome mapping to *Saccharomyces cerevisiae*) between chromosomes across all environments. Inset depicts the distribution of DCH for all chromosome interactions. DCH is determined for each chromosome interaction by taking the difference between the hybridity measurements for each chromosome within an F2 genome (*n* genomes = 237). These values are then averaged across all diploid F2 genomes, and medians and means are reported and colored accordingly. A large DCH (green) suggests that the chromosomes map primarily to opposing species. A small DCH (brown) suggests that the chromosomes have similar levels of hybridity. These chromosomes may come from primarily the same species or at least have similar hybridity proportions. (*B*) Average change in chromosome hybridity between chromosomes for each environment. Calculations are performed the same as panel (*A*) for each environment independently (*n* genomes ~ 24).

range (0.29–0.36) expected from simulations based on no chromosome interactions (fig. 4). Four environments (NaCl: 0.21, hydrogen peroxide: 0.22, lithium acetate: 0.22, DMSO: 0.24) exhibited lower mean DCH than the simulated expected range. An analysis of published data in an environment without added stress (Kao et al. 2010) found slightly higher mean DCH (0.42) than the simulated range (supplementary fig. S6*C*, Supplementary Material online).

Analyzing directional correlations between hybridities of chromosomes within a genome revealed similar environment-dependent interactions (fig. 5). Significant positive correlations suggest positive epistatic interactions within species, meaning that as chromosome hybridity in one chromosome shifted toward one species (1 = *S. cerevisiae*, 0 = *S. paradoxus*), the chromosome hybridity in the linked chromosome also shifted toward the same species (fig. 5*A*). Inversely, negative correlations suggested negative epistatic

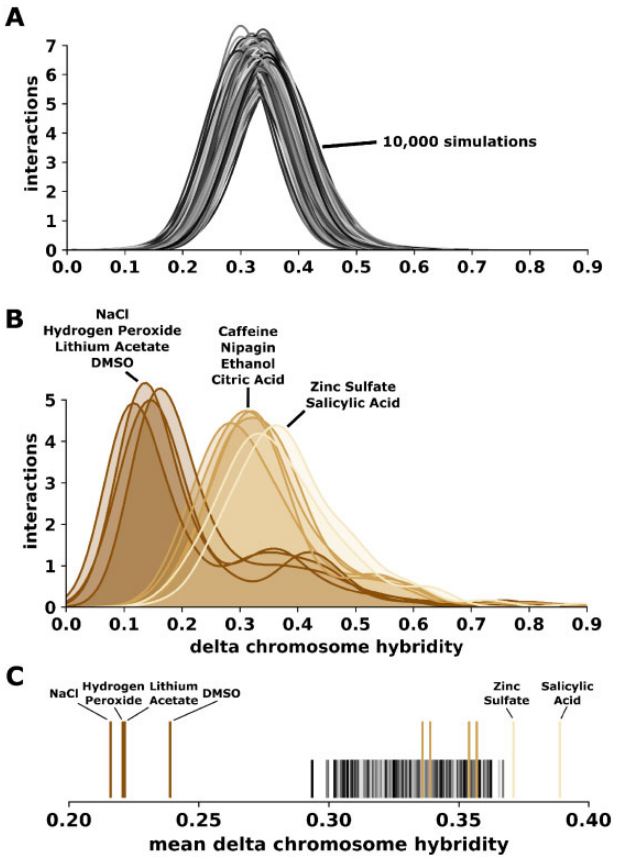

FIG. 4. DCH of simulated chromosomes. (*A*) The distribution of DCH in a simulated environment resulting from simulated chromosomes based on no chromosomal interactions. Each environment consists of 24 genomes, each consisting of 16 simulated chromosomes. Each simulated environment was repeated 10,000 times. (*B*) The distribution of DCH found in our experimental environments. Distributions are colored according to their mean DCH. (*C*) Mean DCH of our experimental environments as compared with the range of mean DCH found in simulations (gray-black lines).

interactions within species. A lack of correlation suggested no significant epistatic interaction. For all environments combined and individually, the distribution of correlations was approximately normal with a mean near zero. There was a range of significant correlations ($P < 0.01$) found across environments ranging in numbers from 0 in salicylic acid and citric acid to 11 in NaCl (fig. 5*B*). The distributions and means for each environment all fell within the range (−0.05 to 0.10) that was expected from simulations based on no chromosome interactions (supplementary fig. S9, Supplementary Material online). However, although the distributions and means were within the range simulated, three environments (lithium acetate: 7, caffeine: 8, and NaCl: 11) exhibited more significant correlations ($P < 0.01$) than the range expected (0–7, supplementary fig. S10, Supplementary Material online). The NaCl environment resulted in a total of 11 significant hybridity correlations (8 positive, 3 negative), whereas 10,000 simulations never encountered more than seven correlations by chance. Interestingly, the NaCl environment also contained the highest molarity range (0.234–0.4 M). However, this correlation between stress concentration and interactions was not found in all environments. Analysis of published data in an environment without stress (Kao et al. 2010) found only a single significant correlation ($P < 0.01$, supplementary fig. S6*D*, Supplementary Material online).

Genotype × Environment Interactions and Gene Ontology

Sampling all F2 hybrid genomes, a total of 315 10-kb bins fixed for either *S. cerevisiae* or *S. paradoxus* were detected (406 bins including chromosomes 5 and 7; supplementary fig. S11*A*, Supplementary Material online). We found large variation between environments ranging from 36 regions in salicylic acid to 372 regions in NaCl. Seventy-eight of these regions were environment-specific, that is, they were inherited from either *S. cerevisiae* or *S. paradoxus* across all 24 hybrid genomes per environment, but only found in one environment.

We identified 1,884 genes that were either located in or overlapped with the 315 fixed regions, ranging from 51 genes in salicylic acid to 1,533 genes in NaCl (supplementary fig. S11*C*, Supplementary Material online). The large differences between environments in the number of fixed alleles suggest that some stress conditions require more complex, quantitative adaptations with a polygenic basis, which is well-known to be the case for yeast adapting to salt for instance (Cubillos et al. 2011; Dhar et al. 2011). Gene annotation analysis showed that most of the 1,884 genes are involved in transport and pathways related to fungal cell-wall organization (supplementary fig. S11*B*, Supplementary Material online). Across environments, we found almost three times more genes fixed for the *S. cerevisiae* allele ($n = 1{,}373$) than fixed for the *S. paradoxus* allele ($n = 511$). Only the F2 hybrid genomes isolated from salicylic acid showed more genes fixed for *S. paradoxus* (46 of 51 genes in total).

Only one region was consistently inherited from *S. cerevisiae* across all environments (chromosome 4: 970,000–980,000 bp, harboring five genes), and one from *S. paradoxus* across all environments (chromosome 15: 10,000–20,000 bp, harboring seven genes). Among these are two general stress response genes, *HSP78* and *PAU20*. *HSP78* on chromosome 4 is associated with heat stress and mitochondrial genome maintenance (Leonhardt et al. 1993; von Janowsky et al. 2006). *PAU20* on chromosome 15 is associated with proteome stress and is upregulated during wine fermentation (Rossignol et al. 2003; Marks et al. 2008; Luo and van Vuuren 2009). It is surprising to find the *S. paradoxus* allele of *PAU20* fixed across all environments as we might expect the *S. cerevisiae* allele to provide higher fitness, especially in fermentation environments.

We did not identify fixations of alternative alleles at the same locus in different environments (e.g., a bin that was consistently inherited from *S. cerevisiae* across all 24 hybrid genomes in ethanol but from *S. paradoxus* in salicylic acid).

Discussion

Hybrid fitness varies among genotypes, generations, and environments (Nolte and Tautz 2010; Arnold et al. 2012; Stelkens,

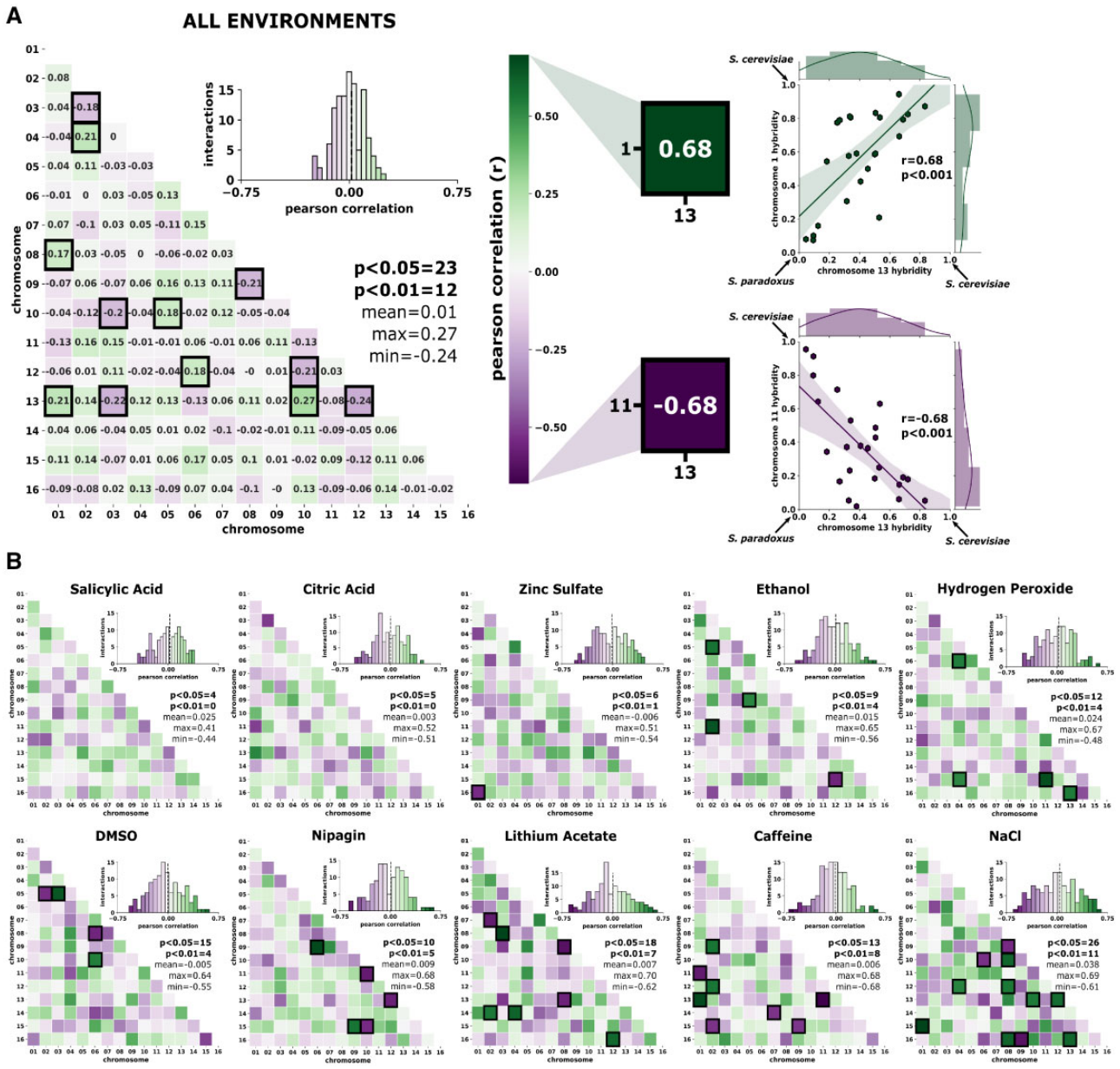

FIG. 5. Epistatic interactions between chromosome hybridity across environments. (*A*) Pearson correlation coefficient (*r*) of chromosome hybridity (percent chromosome mapping to *Saccharomyces cerevisiae*) between chromosomes across all environments (n genomes = 237). Inset depicts the distribution of Pearson correlation coefficients for all chromosome interactions. Positive correlations are shown in green and negative correlations are shown in purple. Statistically significant correlations ($P < 0.01$) are highlighted in black. Examples of strong correlations are shown for the interactions between chromosomes 13 and 11 (positive) and chromosomes 13 and 1 (negative) in the Caffeine environment. (*B*) Pearson correlation between chromosome hybridity within each environment. Calculations are performed as in panel (*B*) but for each environment independently ($n \sim 24$ genomes). Environments are sorted from top left to bottom right according to the number of significant ($P < 0.01$) correlations found.

Brockhurst, Hurst, Miller, et al. 2014; Hwang et al. 2016), but the genetic basis of hybrid fitness is usually unknown, especially in nondomesticated organisms (but see Rieseberg et al. 1999; Payseur and Rieseberg 2016). In addition, the interaction between the environment and the targets of selection in hybrid genomes remains almost entirely unexplored (but see Shahid et al. 2008; Hwang et al. 2016). Whether or not the variation contained in hybrid populations contributes to adaptive evolution crucially depends on the type of genetic mechanism underlying fitness. Under heterozygote advantage, for instance, the most fit genotype cannot breed true in sexual, diploid populations because segregation will inevitably break up beneficial allelic combinations (Buerkle and Rieseberg 2008). But if the most fit genotype is homozygous for alleles derived from each lineage at different loci, such recombinant homozygotes can breed true, may become fixed through drift or selection, and potentially establish new lineages (Fitzpatrick and Shaffer 2007).

Here, we describe the composition of 237 stress-resistant F2 hybrid genomes, made from two divergent *Saccharomyces*

yeast species. We measured variance in overall hybridity, interspecific heterozygosity, and epistasis found between and within hybrid genomes. We found that the composition of hybrid genomes was strongly contingent on environmental context. Genomes from different environments varied in every aspect of hybridness measured. First, genomes from different environments differed in the proportion of interspecific heterozygosity. Although some environments clearly selected for more homozygous genomes (e.g., zinc sulfate), others selected for more heterozygous genomes (e.g., NaCl; fig. 1*B*). Second, individual chromosomes exhibited strong species biases depending on the type of stress they were exposed to (fig. 2*B*). This is presumably because genes important for resistance to the specific toxin are located on these chromosomes, and alleles from parental species differ in how well they tolerate this toxin (supplementary fig. S8, Supplementary Material online). However, we did not observe fixation of opposite species alleles in different environments (supplementary fig. S11, Supplementary Material online). Third, we found evidence for environment-dependent, nonhomologous chromosomal associations (fig. 3). Positive same-species and to our surprise, also positive opposite-species chromosome associations occurred, depending in frequency and in type on the environment (fig. 5). Computer simulations in a selection- and epistasis-free space with independently segregating chromosomes (fig. 4 and supplementary figs. S7, S9, and S10, Supplementary Material online), and a comparison to hybrid genomes grown in a stress-free environment from Kao et al. (2010) (supplementary fig. S6, Supplementary Material online), produced a smaller number of significant associations between chromosomes in hybrid genomes. This suggests that some heterospecific chromosomal combinations were indeed under positive epistatic selection. It is difficult to distinguish between environmental selection and the effects of (nonlethal) genetic incompatibility in our hybrids. However, the analyses of hybrids grown without stress (supplementary fig. S6, Supplementary Material online) suggest that at least a portion of the effect is driven by environmental selection.

Beneficial interactions between genetic materials from species with such large evolutionary divergence (~15%) are surprising. At this genetic distance, which is roughly three times larger than the distance between humans and chimpanzees, hybrid genomes are expected to contain Dobzhansky–Muller incompatibilities (or strong negative epistasis) and other negative fitness effects as a result of species divergence and reproductive isolation. In yeast, the missegregation of chromosomes due to antirecombination (Greig et al. 2003) is probably responsible for most of the >99% mortality observed in the F1 hybrid gametes of *S. cerevisiae* × *S. paradoxus* crosses (Liti et al. 2006; Hou et al. 2014). It is important to keep in mind that we only sampled from the 1% viable subset of all F2 hybrids here, thus a priori excluding lethal hybrids or those with strongly compromised fitness. Still, we might expect selection to favor mainly same-species chromosomal combinations, which is not what we observed here (in the resolution possible given limited rounds of segregation and recombination in the F2 generation).

Interestingly, when screening for recessive incompatibilities in the same hybrid cross, a previous study found that replacing chromosomes 4, 13, and 14 in *S. cerevisiae* with homologous chromosomes from *S. paradoxus* did not yield any viable haploids (Greig 2007). In our experiment, focusing here on the NaCl environment because it revealed the most significant epistatic interactions, the same three chromosomes (4, 13, and 14) were involved in five of eight positive same-species interactions, suggesting that different-species combinations with any of these three chromosomes may indeed cause low fitness in hybrid genomes, and are selected against (fig. 5*B*). In addition, we found three positive opposite-species associations in NaCl involving five chromosomes to occur more often than expected by chance (6, 8, 9, 10, and 16). Of these, Greig (2007) also found four chromosomes (6, 8, 9, and 10) not to be problematic to transfer into the opposite species background (there was no suitable auxotrophic marker for chromosome 16, so this was a technical limitation, not an incompatibility). This is consistent with positive heterospecific epistasis, or at least an absence of incompatibilities on these chromosomes.

Individual chromosomes also differed in their level of interspecific heterozygosity independently of the environment. For instance, chromosomes 4, 6, and 14 were more beneficial to fitness as homozygotes, whereas chromosomes 2, 3, and 12 were more beneficial as heterozygotes (fig. 1*C*). Overall however, interspecific heterozygosity was unexpectedly low across all hybrid genomes (supplementary fig. S1, Supplementary Material online), suggesting that same-species allelic combinations (homozygosity) in an otherwise hybrid genomic background can provide high fitness. These results speak against strong effects of dominance or overdominance to hybrid fitness and are more consistent with directional selection for one of the parental alleles, or selection against heterozygotes (underdominance), which has been shown in *Saccharomyces* (Laiba et al. 2016), natural *Populus* (Lindtke et al. 2012), and *Helianthus* hybrid populations (Lai et al. 2005). Yet, dominance complementation of recessive alleles and overdominant interactions within loci are often reported from laboratory crosses of *Saccharomyces* where heterozygotes are fitter than both homozygotes (Zörgö et al. 2012; Plech et al. 2014; Shapira et al. 2014; Blein-Nicolas et al. 2015; Laiba et al. 2016). In some cases, this inconsistency with our results may be explained by the much smaller genomic divergence (usually <1%) between the parental lineages used in these studies (mostly all *S. cerevisiae* strains). Studies using the same genetically divergent *S. cerevisiae* × *S. paradoxus* cross as us suggested that heterosis in F1 hybrids was likely a result of dominance complementation of recessive deleterious alleles, but may also be due to additional overdominant or epistatic effects (Zörgö et al. 2012; Bernardes et al. 2017). The excess of homozygosity in our experiment is also consistent with many if not most high fitness alleles being recessive and only becoming expressed in the homozygous state. Alternatively, selection on some aspects of fitness in the haploid phase (during sporulation and germination) may have caused strains with the same beneficial combinations of parental chromosomes to mate, resulting in homozygous diploids.

For instance, strains may be able to maximize their fitness by germinating early (Miller and Greig 2015; Stelkens et al. 2016), which could result in a process similar to assortative mating.

Aneuploidy, the gain or loss of chromosomes, is a common byproduct of missegregation in the F1 hybrid meiosis of interspecific yeast crosses (Hunter et al. 1996). We detected high levels of aneuploidy in our F2 hybrid genomes across all environments (208 of 237 genomes contained aneuploidy; supplementary figs. S2 and S3, Supplementary Material online) with significant variation between chromosomes. This may suggest that gene dosage effects due to copy number changes may have helped some hybrids in our experiment survive stress. Aneuploidy is known to be associated with stress and drug resistance in yeast and other fungi (Selmecki et al. 2009; Pavelka et al. 2010; Kwon-Chung and Chang 2012; Yang et al. 2019), and has been suggested to serve as a transient adaptation mechanism (Chang et al. 2013; Hose et al. 2015; Smukowski Heil et al. 2017). In our experiment, chromosome 2, 4, 13, and 14 showed high overall levels of aneuploidy, suggesting that aneuploidy of these chromosomes might be advantageous in stressful environments (supplementary fig. S2*C* and *D*, Supplementary Material online). Chromosome 4 and 13 aneuploidy has been shown to result from hydrogen peroxide (Linder et al. 2017) and galactose stress (Sirr et al. 2015), respectively. Inversely, the low aneuploidy in chromosomes 5 and 7 was likely linked to the selective drug markers located on these chromosomes, which we used to select for F2 hybrids. Interestingly, we did not find a negative correlation between chromosome size and rate of aneuploidy as previously suggested (Gilchrist and Stelkens 2019).

Hybridization mostly occurs at the margins of species ranges where conditions are more extreme than in the center of their distribution, that is, in more stressful environments. Hybridization also occurs more frequently in human- or otherwise perturbed habitats, where geographic and ecological species barriers are lost or weakened (King et al. 2015; Arnold 2016; Gompert and Buerkle 2016; McFarlane and Pemberton 2019). Thus, the circumstances leading to hybridization often coincide with times of increased environmental stress, which in turn creates ecological opportunity. The large number of significant chromosome-by-environment interactions we found in our hybrid populations illustrates the genetic variation typical for hybrid swarms. This can facilitate their functional diversification and, potentially, the colonization of novel and challenging environments as shown for instance in *Helianthus* sunflowers and African cichlid fish (Rieseberg et al. 2003; Seehausen 2004; Abbott et al. 2013). We acknowledge that the facultative asexual reproduction and the ability of yeast to self-fertilize (hybrids do not rely on backcrossing with the parents) can help restore fitness quickly after outbreeding depression in the F2 hybrid generation. Together, this can catalyze the propagation of hybrid genotypes even with small and temporary fitness advantages.

In conclusion, understanding the environmental and genetic mechanisms responsible for hybrid fitness is essential for any predictions regarding the role of hybridization in adaptive evolution (Gompert and Buerkle 2016). For instance, our data suggests that each environment selects for different parental alleles and, also, for different epistatic interactions. Thus, a given hybrid could outcompete and drive a parent population to extinction in one locality, but may have inferior fitness in a different habitat, posing no threat to the parental lines. The results of our study show that in order to capture the risks and benefits of genetic exchange between lineages, it is important to measure multiple dimensions of hybridity and measure hybrid fitness in multiple environmental contexts.

Materials and Methods

Parent and F1 Hybrid Strains

We chose two genetically tractable laboratory strains as parents: *S. cerevisiae* haploid strain YDP907 (*MATα*, *ura3::KanMX*, *can1r*), isogenic with strain background S288c, was crossed to *S. paradoxus* strain YDP728 (*MATa*, *ura3::KanMX*, *cyh2r*), which is isogenic with strain background N17. This produced a diploid F1 hybrid (MATa/@, *ura3::KanMX*, *cyh2r*, *can1r*), which was purified by streaking and then stored frozen at −80 °C in 20% glycerol stock.

F2 Hybrids

To make F2 hybrids, we grew a 5-ml culture of the F1 hybrid in YEPD (1% yeast extract, 2% peptone, 2% dextrose) for 24 h at 30 °C, and then transferred 200 μl of this to 50 ml of KAC sporulation medium (1% potassium acetate, 0.1% yeast extract, 0.05% glucose, 2% agar) which was shaken at room temperature for 5 days to induce meiosis and sporulation. Sporulation was confirmed under the microscope. Fifty microliters of the spore culture, in serial dilutions and using three replicates per dilution, was then plated onto arginine drop-out agar plates supplemented with the drugs canavanine (60 mg/l) and cycloheximide (3.33 mg/l). These drugs kill the fully heterozygous F1 hybrids because the resistance alleles *cyh2r* and *can1r* are recessive. But those meiotic spores (produced by the F1 hybrid) that contain both resistance alleles can, if viable, germinate and form colonies. This method ensured that only viable F2 hybrids were sampled and sequenced.

Environments and Stress

Fifty microliters of spore culture (containing 25.5 double drug-resistant viable spores on average confirmed by streaking out on double-drug medium) was used as the founding population for inoculation and growth on flat-bottomed, 96-well cell culture plates. Wells contained liquid minimal medium plus uracil, cycloheximide, and canavanine (0.67% yeast nitrogen base without amino acids, 2% glucose, 2% agar, 0.003% uracil, 60 mg/l canavanine, 3.33 mg/l cycloheximide), allowing for the germination, mating, and growth of the double drug-resistant F2 progeny. This was supplemented with a range of concentrations of ten toxins (one at a time): salicylic acid ($C_7H_6O_3$), caffeine ($C_8H_{10}N_4O_2$), ethanol (C_2H_6O), zinc sulfate ($ZnSO_4$), hydrogen peroxide (H_2O_2), methyl paraben ("Nipagin"; $CH_3(C_6H_4(OH)COO)$, sodium chloride (NaCl), lithium acetate (CH_3COOLi), dimethyl sulfoxide ("DMSO"; C_2H_6OS), and citric acid ($C_6H_8O_7$). These ten toxins are

arbitrary but do represent established stress environments for yeast, which we have used in previous assays (Stelkens, Brockhurst, Hurst, Miller, et al. 2014; Bernardes et al. 2017). Toxicity gradients (or "environmental clines") were generated along the *y*-axis of the 96-well plates such that the bottom row contained the lowest concentration, and the top row contained the highest concentration of the toxin, lethal for all strains (exact concentrations in supplementary table S1, Supplementary Material online).

Plates were incubated at 30 °C for 4 days. Then, 1 μl from each well was transferred to the same position on a new 96-well culture plate containing identical concentrations. The optical density (OD) of each well was measured with a microplate reader (Infinite M200 Pro, Tecan) (time point t_0), and plates were incubated at 30 °C for another 3 days. After this, another OD measurement was taken (t_1) and plates were stored at 4 °C until further processing. We calculated, for each well, whether growth had occurred by subtracting ODt_0 from ODt_1. Assuming that a doubling in OD approximately equals a doubling of cell numbers, cells in permissive environments at the bottom of the plate completed on average three cell cycles (2.78 $\pm$ 0.15 across toxins) from t_0 to t_1 whereas cells in the topmost row did not divide at all.

We sampled from all 12 wells of the bottom row (i.e., the lowest stress) and from the 12 wells of the highest stress that allowed growth from each column, from all ten plates. These 240 samples were streaked out for single colonies on YEPD plates and grown for 48 h at 30 °C. We then picked a single colony from each sample and froze it for sequencing.

DNA Extraction, Polymerase Chain Reaction, and Sequencing Protocols

DNA was extracted using the MasterPure Yeast DNA Purification Kit (Epicentre). A genotyping-by-sequencing protocol was modified from microsatellite library preparation and ddRAD sequencing approaches as follows (Nolte et al. 2005; Peterson et al. 2012). The library construction is based on an efficient combined restriction digest/adaptor ligation. The restriction enzymes *Csp*6I (which cleaves 5′-G̲T A C-3′ sites) and *Pst*I (which cleaves 5′-C T G C A̲G-3′ sites) were used to digest genomic DNA to generate sticky ends. The reaction conditions permit that sticky end adapters and T4 ligase are added to the reaction such that adaptors are ligated to the restriction sites. Importantly, the adaptors do not fully reconstitute the restriction sites. Thus, once an adaptor is ligated, this site will not be recut whereas an undesired ligation of two genomic DNA sticky ends will be recut until all DNA ends are saturated with an adaptor. For this purpose, we modified the ligation sites of the Illumina Truseq adapters such that they matched the sticky ends generated by the restriction enzymes. Further, we labeled the adapters to include 24 and 16 different molecular barcodes (MIDs), respectively, which could be combined in 384 different combinations for multiplexed sequencing (paired ends) of the libraries on an Illumina MiSeq sequencer.

Quality Filtering of Raw Reads and Mapping Protocol

We examined the quality of raw ddRADseq reads of each sample using FastQC (v0.11.8) (FastQC 2018). Illumina sequencing adapters, primer sequences, ambiguous, and low-quality nucleotides (PHRED quality score $<$ 20) were removed from both paired-end reads according to the default parameters in the NGS QC Toolkit (v2.3.3) (Patel and Jain 2012). Three of 240 F2 genomes were abandoned due to low sequence yield. A total of 8.2-Gb high-quality reads were generated after quality control with mean depth of 12.84 per marker. Sequencing data are available at the European Nucleotide Archive (ENA accession number: PRJEB33368).

Parental strain sequences were downloaded from the *Saccharomyces* Genome Database website. The S288c reference genome used was R64-2-1_20150113. The N17 reference genome was obtained from ftp://ftp.sanger.ac.uk/pub/users/dmc/yeast/latest/, in the para_assemblies/N_17 folder.

Given the high sequence divergence between *S. cerevisiae* and *S. paradoxus* (15%), correct assignment of reads to the parental species was efficient using NovoAlign (NovoAlign 2018) with default parameters. For this, both parental genomes were concatenated and used as a combined reference for mapping, and species affiliations and chromosomal positions of successfully mapped reads were written to the same output file. Mapped reads were considered correctly assigned to the reference sequence when the mapping quality was $\geq$20, indicating a single and unique best match.

Ploidy Determination

To differentiate haploid and diploid F2 hybrid genomes (to be able to score the prevalence of homo- and heterozygosity), we mapped paired-end reads again, this time only to the *S. cerevisiae* S288c reference genome using NovoAlign (NovoAlign 2018) with the default parameters. We sorted mapped files according to their genomic coordinates using Picard Tools v2.18.23 (Picard 2019) and performed variant calling in FreeBayes (Garrison and Marth 2012) with at least five supporting reads required to consider a variant. Single nucleotide polymorphisms were selected and filtered using GATK (Li et al. 2008) according to stringent filtering criteria with the following settings: 1) quality $>$ 30.0, 2) quality by depth $>$ 5.0, 3) fisher strand $<$ 60.0, 4) root mean square of mapping quality $>$ 40.0, 5) MQRankSum $>$ $-$12.5; and 6) ReadPosRankSum $>$ $-$8.0. Additionally, if there were more than three SNPs clustered in a 10-bp window, we considered all three SNPs false positives and removed them. After filtering, we identified 14,975 SNPs, ranging between 10,725 and 12,345 among environments.

Haploidy or diploidy was called using the heterozygosity score of biallelic SNPs using a custom bash script. Theoretically, both the number of heterozygous SNPs and ratio of heterozygous SNPs over the total SNPs in haploids should be zero (except in case of sequencing errors and aneuploidies). However, the absolute number of heterozygous SNPs is affected by the overall sequence size of each sample, and the ratio is affected by the number of SNPs derived from *S. paradoxus* (because of the large nucleotide divergence between the parents, ~15% of the reads from *S. paradoxus* do

not map to the *S. cerevisiae* reference genome). Also, although unlikely, diploid F2 genomes can theoretically be fully homozygous with both copies of eight chromosomes inherited from each parental species, assuming that genetic material from both parental species is equally represented in the F2 generation. At zero heterozygosity, haploid and diploid genomes are indistinguishable by SNP calling and mapping to parental genomes. Thus, at the risk of omitting extremely homozygous diploids, we applied two criteria to consider a genome diploid: 1) The number of heterozygous SNPs in a diploid F2 genome should be larger than the average number of heterozygous SNPs found in both parental genomes, and 2) the ratio of heterozygous over hetero- plus homozygous SNPs in a diploid F2 genome should be larger than the average ratio of heterozygous over hetero- plus homozygous SNPs in parental genomes. As there are nearly zero heterozygous SNPs in the *S. cerevisiae* genome, this can be simplified to:

$$\text{ratio}\left(\text{SNP}^{\text{hetero}}_{\text{extreme}}\right) \approx \frac{\frac{n\left(\text{SNP}^{\text{hetero}}_{S.par}\right)}{n\left(\text{SNP}^{\text{hetero}}_{S.par}\right)+n\left(\text{SNP}^{\text{homo}}_{S.par}\right)}}{2}.$$

Using this analysis, we assigned 187 of the 237 F2 genomes to be diploid.

Chromosome Copy Number

To calculate chromosome copy number, the same mapping files used for ploidy determination of each genome were divided into 10-kb bins. Next, a series of filtering steps were performed to select an optimal set of bins to represent the chromosome copy number across the genome. To eliminate sequencing and fragmentation error, we first removed bins with a median read depth <2 in the nine euploid F1 hybrids and each F2 genome sequenced for this study. Then, the proportion of all reads aligning to that bin was calculated using a previously described method (Tan et al. 2013):

$$\text{Bin proportion} = \frac{\text{Read counts for bin}}{\text{Total read counts for strain}}.$$

To eliminate bin-specific coverage effects, for each bin in each query F2 strain, the bin proportion was normalized using the mean bin proportion of the same coordinate from the nine euploid F1 hybrids:

$$\text{Bin ratio} = \frac{\text{Query bin proportion}}{\text{Mean bin proportion of 9 F1 hybrids}}.$$

This ratio at the 10-kb bin level still showed sequencing bias as a result of the ddRAD sequencing approach, for example, chromosome-end bias, GC-content bias, fragment-length bias, etc. Considering that the effects of these biases are likely minimal at the chromosome level, we then calculated the chromosome ratio of each query strain and normalized the median chromosome ratio to 2 in diploids, or to 1 in haploids:

$$\text{Chromosome ratio}_{\text{Query strain normalized}} = \frac{\text{Chromosome ratio}}{\text{Median chromosome ratio for query strain}}.$$

After that, we transformed the 10-kb bin ratio using BoxCox (Box and Cox 1964) and normalized the data using the chromosome ratio. This was then used to represent the chromosome copy number:

$$\text{Chromosome copy number} = \text{Bin ratio}_{\text{BoxCox}} \times \text{Chromosome ratio}_{\text{Query strain normalized}}.$$

Chromosome Zygosity

To determine the zygosity of each chromosome in diploid F2 genomes, we mapped high-quality reads of each sample to the reference combining both parental genomes. We extracted the species affiliation of each read using a custom bash script. The chromosomal content per species per sample was extracted using custom perl code by calculating the proportion of markers mapping to only one species over markers mapping to both species. We considered chromosomes heterozygous if marker proportions fell between 0.25 and 0.75. Chromosomes with smaller or larger species content were assigned homozygous.

To understand what causes variation in zygosity between environments, chromosomes, and genomes, we modeled chromosome heterozygosity using a mixed-effect linear model. Chromosome zygosity was used as the response variable in the model and was predicted as a function of fixed predictors environment and chromosome ID and their interactions and sample ID as a random effect. We selected the most appropriate model by identifying the simplest model that maintained the lowest Akaike Information Criterion (AIC; Akaike 1974). AIC optimizes the relationship between the fit and complexity of a model by balancing the fit of the model with the number of parameters estimated (Harrison et al. 2018).

Genome-Level and Chromosome-Level Hybridity

To describe the genome-level and chromosome-level hybridity, we calculated the percentage of the entire genome or chromosome for each sample that mapped to either the *S. cerevisiae* or the *S. paradoxus* genome. We defined hybridity as the percent of markers per genome or chromosome mapping to *S. cerevisiae* (100% = *S. cerevisiae*, 0% = *S. paradoxus*). This was calculated across all environments, as well as for each environment individually. We then used mixed-effect linear models with genome and chromosome hybridity as response variables. We predicted hybridity to be a function of the fixed effects *aneuploidy*, *environment*, *chromosome ID*, *ploidy*, and their interactions and included sample ID as random effect. We selected the most appropriate model by starting with the full model and removing insignificant components, identifying the simplest model that maintained the lowest AIC.

To characterize the interactions between chromosomes within a F2 genome, we calculated the difference in chromosome hybridity for each chromosome combination, defined as DCH. Large DCH indicates that the two chromosomes map primarily to opposing species within a genome. Small DCH indicates that the chromosomes have similar levels of

hybridity, suggesting that either the chromosomes come from primarily the same species or at least they have similar hybridity proportions. DCH was calculated for all environments together, as well as each environment individually. To investigate the epistatic interactions between chromosomes, we determined the Pearson correlation (r) between chromosome hybridity for all pairwise chromosome combinations. A significant positive correlation between two chromosomes suggests a positive epistatic interaction within a species, meaning that as chromosome hybridity in one chromosome shifts toward one species (1 = *S. cerevisiae*, 0 = *S. paradoxus*), the chromosome hybridity in the linked chromosome also shifts toward the same species. A significant negative correlation between two chromosomes suggests a negative epistatic interaction within a species. In this case, as one chromosome shifts toward one species, the linked chromosome shifts toward the other species. Custom Python scripts used for analyses of hybridity are available on GitLab (https://gitlab.com/devinbendixsen/yeast_hybrid_stress).

Simulated Chromosomes

In order to determine whether the observed zygosity, hybridity, and chromosomal interactions found in each environment deviated from neutral expectations, we developed simulations that determined the expected range for these measurements based solely on chance, assuming no selection and free segregation of chromosomes in hybrid genomes. Each simulation displayed the expected distribution of zygosity, hybridity, or chromosomal interactions that could be found in a selection-free environment with no epistasis between chromosomes. Each simulated environment was repeated 10,000 times. Each environment consisted of 24 genomes and each genome consisted of 16 chromosomes as found in our data. Each chromosome was randomly assigned a chromosome hybridity score between 0 and 1. To study the expected zygosity, chromosomes were labeled as either homozygous for *S. cerevisiae* or *S. paradoxus* or heterozygous based on the same rules used in the analysis of our data (see Chromosome Zygosity). The heterozygosity and hybridity for each genome were then calculated for each simulation. The means and distributions of these values were plotted and compared with the means and distributions we received from our data (supplementary figs. S1 and S7, Supplementary Material online). To study the expected chromosome interactions, we calculated the 120 interactions that occur within a simulated genome between chromosomes. DCH and Pearson correlation (r) were calculated in the same manner as our data was analyzed (see Genome-Level and Chromosome-Level Hybridity). The distributions of these interactions were then plotted and compared with the data from our study (fig. 4 and supplementary fig. S9, Supplementary Material online). For the Pearson correlation (r), we also determined the range of expected significant positive and negative correlations and compared them with our data (supplementary fig. S10, Supplementary Material online). Custom Python scripts used for simulations are available on GitLab (https://gitlab.com/devinbendixsen/yeast_hybrid_stress).

Genotype × Environment Interactions and Gene Ontology

To explore for gene-by-environment interactions, that is, which gene from which species background is more frequently found in which environment, we divided genomes into 10-kb bins. Assuming each bin is a locus and the parental species affiliations are the two possible alleles, we scored bins as 1 if all markers within that bin mapped to the *S. cerevisiae* reference genome, and 0 if all markers mapped to the *S. paradoxus* reference genome across all 24 genomes within a given environment (excluding chromosome 5 and 7). Genes located in or overlapping with these fixed regions of each environment were further inspected using the gene annotation data base DAVID (Huang et al. 2009). Environment-independent fixations of alleles (bins fixed for the same species across all environments) and unique fixations (bin fixed only for one environment) were extracted using custom R code.

Analysis of Hybrid Genomes in Environment without Toxin

Data from *S. cerevisiae* × *S. paradoxus* F2 hybrids grown in an environment without any toxin were obtained from Kao et al. (2010). These data were generated using a dual-species comparative genomic hybridization microarray analysis with species-specific DNA oligos for *S. cerevisiae* and *S. paradoxus*. Data for 36 hybrid genomes were analyzed by first determining the number of oligos that mapped significantly to each species (using LOG_RAT2N_MEAN = −0.05 as a cut-off). Genome and chromosome hybridity (defined as percentage of oligos mapping to *S. cerevisiae*) were calculated (supplementary fig. S6*A* and *B*, Supplementary Material online). DCH and Pearson correlation were analyzed as previously described for our own data (supplementary fig. S6*C* and *D*, Supplementary Material online). Custom Python scripts used for these analyses are available on GitLab (https://gitlab.com/devinbendixsen/yeast_hybrid_stress).

Supplementary Material

Supplementary data are available at *Molecular Biology and Evolution* online.

Acknowledgments

We thank Elke Bustorf for the preparation of libraries and David Rogers for advice on mapping. We also thank Katy C. Kao for providing data for hybrids that were grown in an environment without toxin. This work was supported by the Max Planck Society (to D.G.), ERC Starting Grant ("EVOLMAPPING" to A.W.N.), Swedish Research Council (Grant Number 2017-04963 to R.S.), Knut and Alice Wallenberg Foundation (Grant Number 2017.0163 to R.S.) Carl Trygger Foundation (to Z.Z.), and Wenner-Gren Foundation (Grant Number UPD2018-0196 to D.P.B.).

Author Contributions

R.S. and D.G. received the project idea and designed the experiment. R.S. performed the experiment and collected the samples. A.W.N. planned and performed the library

preparation and sequencing. Z.Z. processed the ddRADseq data. Z.Z., D.P.B., and T.J. analyzed the data. R.S., Z.Z., and D.P.B. wrote the manuscript.

References

Abbott R, Albach D, Ansell S, Arntzen JW, Baird SJE, Bierne N, Boughman JW, Brelsford A, Buerkle CA, Buggs R. 2013. Hybridization and speciation. *J Evol Biol*. 26(2):229–246.

Akaike H. 1974. A new look at the statistical model identification. *IEEE Trans Automat Contr*. 19(6):716–723.

Anderson E, Stebbins GL. 1954. Hybridization as an evolutionary stimulus. *Evolution* 8(4):378–388.

Armbruster P, Bradshaw WE, Steiner AL, Holzapfel CM. 1999. Evolutionary responses to environmental stress by the pitcher-plant mosquito, *Wyeomyia smithii*. *Heredity* 83(5):509–519.

Arnold ML. 2006. Evolution through genetic exchange. Oxford/New York: Oxford University Press.

Arnold ML. 2016. Anderson's and Stebbins' prophecy comes true: genetic exchange in fluctuating environments. *Syst Bot*. 41(1):4–16.

Arnold ML, Ballerini ES, Brothers AN. 2012. Hybrid fitness, adaptation and evolutionary diversification: lessons learned from Louisiana Irises. *Heredity (Edinb)*. 108(3):159–166.

Barreto FS, Burton RS. 2013. Elevated oxidative damage is correlated with reduced fitness in interpopulation hybrids of a marine copepod. *Proc R Soc B*. 280(1767):20131521.

Barton NH. 2000. Estimating multilocus linkage disequilibria. *Heredity* 84(3):373–389.

Barton NH, Gale KS. 1993. Genetic analysis of hybrid zones. In: Harrison RG, editor. Hybrid zones and the evolutionary process. New York: Oxford University Press. p. 13–45.

Bernardes JP, Stelkens RB, Greig D. 2017. Heterosis in hybrids within and between yeast species. *J Evol Biol*. 30(3):538–548.

Blein-Nicolas M, Albertin W, da Silva T, Valot B, Balliau T, Masneuf-Pomarède I, Bely M, Marullo P, Sicard D, Dillmann C, et al. 2015. A systems approach to elucidate heterosis of protein abundances in yeast. *Mol Cell Proteomics*. 14(8):2056–2071.

Box GE, Cox DR. 1964. An analysis of transformations. *J R Stat Soc Series B (Methodol)*. 26:211–243.

Boynton PJ, Janzen T, Greig D. 2018. Modeling the contributions of chromosome segregation errors and aneuploidy to *Saccharomyces* hybrid sterility. *Yeast* 35(1):85–98.

Bruce AB. 1910. The Mendelian theory of heredity and the augmentation of vigor. *Science* 32(827):627.

Buerkle CA. 2005. Maximum-likelihood estimation of a hybrid index based on molecular markers. *Mol Ecol Notes*. 5(3):684–687.

Buerkle CA, Rieseberg LH. 2008. The rate of genome stabilization in homoploid hybrid species. *Evolution* 62(2):266–275.

Chang S-L, Lai H-Y, Tung S-Y, Leu J-Y. 2013. Dynamic large-scale chromosomal rearrangements fuel rapid adaptation in yeast populations. *PLoS Genet*. 9(1):e1003232.

Coyne JA, Orr HA. 2004. Speciation. Sunderland (MA): Sinauer Associates.

Cubillos FA, Billi E, Zörgo E, Parts L, Fargier P, Omholt S, Blomberg A, Warringer J, Louis EJ, Liti G. 2011. Assessing the complex architecture of polygenic traits in diverged yeast populations. *Mol Ecol*. 20(7):1401–1413.

de Vos MGJ, Poelwijk FJ, Battich N, Ndika JDT, Tans SJ. 2013. Environmental dependence of genetic constraint. *PLoS Genet*. 9(6):e1003580.

Dhar R, Sagesser R, Weikert C, Yuan J, Wagner A. 2011. Adaptation of *Saccharomyces cerevisiae* to saline stress through laboratory evolution. *J Evol Biol*. 24(5):1135–1153.

Dittrich-Reed DR, Fitzpatrick BM. 2013. Transgressive hybrids as hopeful monsters. *Evol Biol*. 40(2):310–315.

Dobzhansky T. 1936. Studies on hybrid sterility. II. Localization of sterility factors in *Drosophila pseudoobscura* hybrids. *Genetics* 21(2):113–135.

Edmands S, Deimler JK. 2004. Local adaptation, intrinsic coadaptation and the effects of environmental stress on interpopulation hybrids in the copepod *Tigriopus californicus*. *J Exp Mar Biol Ecol*. 303(2):183–196.

Falush D, Stephens M, Pritchard JK. 2003. Inference of population structure using multilocus genotype data: linked loci and correlated allele frequencies. *Genetics* 164(4):1567–1587.

FastQC. 2018. Available from: https://www.bioinformatics.babraham.ac.uk/projects/fastqc/, last accessed March 2019.

Filteau M, Hamel V, Pouliot MC, Gagnon-Arsenault I, Dube AK, Landry CR. 2015. Evolutionary rescue by compensatory mutations is constrained by genomic and environmental backgrounds. *Mol Syst Biol*. 11(10):832.

Fitzpatrick BM. 2012. Estimating ancestry and heterozygosity of hybrids using molecular markers. *BMC Evol Biol*. 12(1):131–114.

Fitzpatrick BM, Shaffer HB. 2007. Hybrid vigor between native and introduced salamanders raises new challenges for conservation. *Proc Natl Acad Sci U S A*. 104(40):15793–15798.

Garrison E, Marth G. 2012. Haplotype-based variant detection from short-read sequencing. arXiv:1207.3907v2 [q-bio.GN], last accessed March 2019.

Gilchrist C, Stelkens R. 2019. Aneuploidy in yeast: segregation error or adaptation mechanism? *Yeast*. https://doi.org/10.1002/yea.3427.

Gompert Z, Buerkle CA. 2013. Analyses of genetic ancestry enable key insights for molecular ecology. *Mol Ecol*. 22(21):5278–5294.

Gompert Z, Buerkle CA. 2016. What, if anything, are hybrids: enduring truths and challenges associated with population structure and gene flow. *Evol Appl*. 9(7):909.

Greig D. 2007. A screen for recessive speciation genes expressed in the gametes of F1 hybrid yeast. *PLoS Genet*. 3(2):e21–286.

Greig D, Louis EJ, Borts RH, Travisano M. 2002. Hybrid speciation in experimental populations of yeast. *Science* 298(5599):1773–1775.

Greig D, Travisano M, Louis EJ, Borts RH. 2003. A role for the mismatch repair system during incipient speciation in *Saccharomyces*. *J Evol Biol*. 16(3):429–437.

Harrison XA, Donaldson L, Correa-Cano ME, Evans J, Fisher DN, Goodwin CED, Robinson BS, Hodgson DJ, Inger R. 2018. A brief introduction to mixed effects modelling and multi-model inference in ecology. *PeerJ* 6:e4794.

Holzman R, Hulsey CD. 2017. Mechanical transgressive segregation and the rapid origin of trophic novelty. *Sci Rep*. 7:40306.

Hose J, Yong CM, Sardi M, Wang Z, Newton MA, Gasch AP. 2015. Dosage compensation can buffer copy-number variation in wild yeast. *eLife* 4:e05462.

Hou J, Friedrich A, de Montigny J, Schacherer J. 2014. Chromosomal rearrangements as a major mechanism in the onset of reproductive isolation in *Saccharomyces cerevisiae*. *Curr Biol*. 24(10):1153–1159.

Huang DW, Sherman BT, Lempicki RA. 2009. Systematic and integrative analysis of large gene lists using DAVID bioinformatics resources. *Nat Protoc*. 4(1):44–57.

Hunter N, Chambers S, Louis E, Borts R. 1996. The mismatch repair system contributes to meiotic sterility in an interspecific yeast hybrid. *EMBO J*. 15(7):1726–1733.

Hwang AS, Pritchard VL, Edmands S. 2016. Recovery from hybrid breakdown in a marine invertebrate is faster, stronger and more repeatable under environmental stress. *J Evol Biol*. 29(9):1793–1803.

Jaffe M, Dziulko A, Smith JD, St Onge RP, Levy SF, Sherlock G. 2019. Improved discovery of genetic interactions using CRISPRiSeq across multiple environments. *Genome Res*. 29(4):668.

Kao KC, Schwartz K, Sherlock G. 2010. A genome-wide analysis reveals no nuclear Dobzhansky-Muller pairs of determinants of speciation between *S. cerevisiae* and *S. paradoxus*, but suggests more complex incompatibilities. *PLos Genet*. 6(7):e1001038.

King KC, Stelkens RB, Webster JP, Smith DF, Brockhurst MA. 2015. Hybridization in parasites: consequences for adaptive evolution, pathogenesis, and public health in a changing world. *PLoS Pathog*. 11(9):e1005098.

Koevoets T, Van De Zande L, Beukeboom LW. 2012. Temperature stress increases hybrid incompatibilities in the parasitic wasp genus *Nasonia*. *J Evol Biol*. 25(2):304–316.
Koide Y, Sakaguchi S, Uchiyama T, Ota Y, Tezuka A, Nagano AJ, Ishiguro S, Takamure I, Kishima Y. 2019. Genetic properties responsible for the transgressive segregation of days to heading in rice. G3 (Bethesda). 9:1655–1662.
Kuczyńska A, Surma M, Adamski T. 2007. Methods to predict transgressive segregation in barley and other self-pollinated crops. *J Appl Genet*. 48(4):321–328.
Kvitek DJ, Sherlock G. 2011. Reciprocal sign epistasis between frequently experimentally evolved adaptive mutations causes a rugged fitness landscape. *PLoS Genet*. 7(4):e1002056.
Kwon-Chung KJ, Chang YC. 2012. Aneuploidy and drug resistance in pathogenic fungi. *PLoS Pathog*. 8(11):e1003022.
Lai Z, Nakazato T, Salmaso M, Burke JM, Tang S, Knapp SJ, Rieseberg LH. 2005. Extensive chromosomal repatterning and the evolution of sterility barriers in hybrid sunflower species. *Genetics* 171(1):291–303.
Laiba E, Glikaite I, Levy Y, Pasternak Z, Fridman E. 2016. Genome scan for nonadditive heterotic trait loci reveals mainly underdominant effects in *Saccharomyces cerevisiae*. *Genome* 59(4):231–242.
Lee JT, Coradini ALV, Shen A, Ehrenreich IM. 2019. Layers of cryptic genetic variation underlie a yeast complex trait. *Genetics* 211(4):1469–1482.
Leonhardt SA, Fearson K, Danese PN, Mason TL. 1993. HSP78 encodes a yeast mitochondrial heat shock protein in the Clp family of ATP-dependent proteases. *Mol Cell Biol*. 13(10):6304–6313.
Lewontin RC, Birch LC. 1966. Hybridization as a source of variation for adaptation to new environments. *Evolution* 20(3):315–336.
Li H, Ruan J, Durbin R. 2008. Mapping short DNA sequencing reads and calling variants using mapping quality scores. *Genome Res*. 18(11):1851–1858.
Linder RA, Greco JP, Seidl F, Matsui T, Ehrenreich IM. 2017. The stress-inducible peroxidase TSA2 underlies a conditionally beneficial chromosomal duplication in *Saccharomyces cerevisiae*. *G3 (Bethesda)* 7(9):3177–3184.
Lindtke D, Buerkle CA, Barbará T, Heinze B, Castiglione S, Bartha D, Lexer C. 2012. Recombinant hybrids retain heterozygosity at many loci: new insights into the genomics of reproductive isolation in *Populus*. *Mol Ecol*. 21(20):5042–5058.
Liti G, Barton DBH, Louis EJ. 2006. Sequence diversity, reproductive isolation and species concepts in *Saccharomyces*. *Genetics* 174(2):839–850.
Liti G, Carter DM, Moses AM, Warringer J, Parts L, James SA, Davey RP, Roberts IN, Burt A, Koufopanou V, et al. 2009. Population genomics of domestic and wild yeasts. *Nature* 458(7236):337–341.
Luo Z, van Vuuren HJ. 2009. Functional analyses of PAU genes in *Saccharomyces cerevisiae*. *Microbiology (Reading, Engl)*. 155(Pt 12):4036–4049.
Lynch M. 1991. The genetic interpretation of inbreeding depression and outbreeding depression. *Evolution* 45(3):622–629.
Mallet J. 2007. Hybrid speciation. *Nature* 446(7133):279–283.
Marks VD, Ho Sui SJ, Erasmus D, van der Merwe GK, Brumm J, Wasserman WW, Bryan J, van Vuuren HJ. 2008. Dynamics of the yeast transcriptome during wine fermentation reveals a novel fermentation stress response. *FEMS Yeast Res*. 8(1):35–52.
Marullo P, Bely M, Masneuf-Pomarede I, Pons M, Aigle M, Dubourdieu D. 2006. Breeding strategies for combining fermentative qualities and reducing off-flavor production in a wine yeast model. *FEMS Yeast Res*. 6(2):268–279.
McFarlane SE, Pemberton JM. 2019. Detecting the true extent of introgression during anthropogenic hybridization. *Trends Ecol Evol (Amst)*. 34(4):315–326.
Miller EL, Greig D. 2015. Spore germination determines yeast inbreeding according to fitness in the local environment. *Am Nat*. 185(2):291–301.
Müller HJ. 1942. Isolating mechanisms, evolution and temperature. *Biol Symp*. 6:71–125.
Nolte AW, Freyhof J, Stemshorn KC, Tautz D. 2005. An invasive lineage of sculpins, *Cottus* sp. (Pisces, Teleostei) in the Rhine with new habitat adaptations has originated from hybridisation between old phylogeographic groups. *Proc R Soc B*. 272(1579):2379–2387.
Nolte AW, Tautz D. 2010. Understanding the onset of hybrid speciation. *Trends Genet*. 26(2):54–58.
NovoAlign. 2018. Available from: http://novocraft.com, last accessed March 2019.
Patel RK, Jain M. 2012. NGS QC Toolkit: a toolkit for quality control of next generation sequencing data. *PLoS One* 7(2):e30619.
Pavelka N, Rancati G, Zhu J, Bradford WD, Saraf A, Florens L, Sanderson BW, Hattem GL, Li R. 2010. Aneuploidy confers quantitative proteome changes and phenotypic variation in budding yeast. *Nature* 468(7321):321–325.
Payseur BA, Rieseberg LH. 2016. A genomic perspective on hybridization and speciation. *Mol Ecol*. 25(11):2337–2360.
Peterson BK, Weber JN, Kay EH, Fisher HS, Hoekstra HE. 2012. Double digest RADseq: an inexpensive method for de novo SNP discovery and genotyping in model and non-model species. *PLoS One* 7(5):e37135.
Picard. 2019. Available from: https://broadinstitute.github.io/picard/, last accessed March 2019.
Plech M, de Visser J, Korona R. 2014. Heterosis is prevalent among domesticated but not wild strains of *Saccharomyces cerevisiae*. *G3* 4:315–323.
Pritchard JK, Stephens M, Donnelly P. 2000. Inference of population structure using multilocus genotype data. *Genetics* 155(2):945–959.
Pritchard VL, Knutson VL, Lee M, Zieba J, Edmands S. 2013. Fitness and morphological outcomes of many generations of hybridization in the copepod *Tigriopus californicus*. *J Evol Biol*. 26(2):416–433.
Rieseberg LH, Archer MA, Wayne RK. 1999. Transgressive segregation, adaptation and speciation. *Heredity* 83(4):363–372.
Rieseberg LH, Raymond O, Rosenthal DM, Lai Z, Livingstone K, Nakazato T, Durphy JL, Schwarzbach AE, Donovan LA, Lexer C. 2003. Major ecological transitions in wild sunflowers facilitated by hybridization. *Science* 301(5637):1211–1216.
Rogers DW, McConnell E, Ono J, Greig D. 2018. Spore-autonomous fluorescent protein expression identifies meiotic chromosome mis-segregation as the principal cause of hybrid sterility in yeast. *PLoS Biol*. 16(11):e2005066.
Rossignol T, Dulau L, Julien A, Blondin B. 2003. Genome-wide monitoring of wine yeast gene expression during alcoholic fermentation. *Yeast* 20(16):1369–1385.
Schumer M, Rosenthal GG, Andolfatto P. 2014. How common is homoploid hybrid speciation? *Evolution* 68(6):1553–1560.
Seehausen O. 2004. Hybridization and adaptive radiation. *Trends Ecol Evol (Amst)*. 19(4):198–207.
Selmecki AM, Dulmage K, Cowen LE, Anderson JB, Berman J. 2009. Acquisition of aneuploidy provides increased fitness during the evolution of antifungal drug resistance. *PLoS Genet*. 5(10):e1000705.
Shahid M, Han S, Yoell H, Xu J. 2008. Fitness distribution and transgressive segregation across 40 environments in a hybrid progeny population of the human-pathogenic yeast *Cryptococcus neoformans*. *Genome* 51(4):272–281.
Shapira R, Levy T, Shaked S, Fridman E, David L. 2014. Extensive heterosis in growth of yeast hybrids is explained by a combination of genetic models. *Heredity (Edinb)* 113(4):316–326.
Shivaprasad PV, Dunn RM, Santos B, Bassett A, Baulcombe DC. 2012. Extraordinary transgressive phenotypes of hybrid tomato are influenced by epigenetics and small silencing RNAs. *EMBO J*. 31(2):257–266.
Sirr A, Cromie GA, Jeffery EW, Gilbert TL, Ludlow CL, Scott AC, Dudley AM. 2015. Allelic variation, aneuploidy, and nongenetic mechanisms suppress a monogenic trait in yeast. *Genetics* 199(1):247–262.
Smukowski Heil CS, DeSevo CG, Pai DA, Tucker CM, Hoang ML, Dunham MJ. 2017. Selection on heterozygosity drives adaptation in intra- and interspecific hybrids. *Mol Biol Evol* 34:1596–1612.

Stelkens RB, Brockhurst MA, Hurst GD, Greig D. 2014. Hybridization facilitates evolutionary rescue. *Evol Appl*. 7(10):1209–1217.

Stelkens RB, Brockhurst MA, Hurst GDD, Miller EL, Greig D. 2014. The effect of hybrid transgression on environmental tolerance in experimental yeast crosses. *J Evol Biol*. 27(11):2507–2519.

Stelkens RB, Miller EL, Greig D. 2016. Asynchronous spore germination in isogenic natural isolates of *Saccharomyces paradoxus*. *FEMS Yeast Res*. 16(3):fow012.

Stelkens RB, Seehausen O. 2009. Genetic distance between species predicts novel trait expression in their hybrids. *Evolution* 63(4):884–897.

Tan Z, Hays M, Cromie GA, Jeffery EW, Scott AC, Ahyong V, Sirr A, Skupin A, Dudley AM. 2013. Aneuploidy underlies a multicellular phenotypic switch. *Proc Natl Acad Sci U S A*. 110(30):12367–12372.

von Janowsky B, Major T, Knapp K, Voos W. 2006. The disaggregation activity of the mitochondrial ClpB homolog Hsp78 maintains Hsp70 function during heat stress. *J Mol Biol*. 357(3):793–807.

Willett CS. 2012. Hybrid breakdown weakens under thermal stress in population crosses of the copepod *Tigriopus californicus*. *J Hered*. 103(1):103–114.

Yang F, Teoh F, Tan ASM, Cao Y, Pavelka N, Berman J. 2019. Aneuploidy enables cross-adaptation to unrelated drugs. *Mol Biol Evol*. 36(8):1768.

Zörgö E, Gjuvsland A, Cubillos FA, Louis EJ, Liti G, Blomberg A, Omholt SW, Warringer J. 2012. Life history shapes trait heredity by accumulation of loss-of-function alleles in yeast. *Mol Biol Evol*. 29(7):1781–1789.